JAAS
Journal of Analytical Atomic Spectrometry

Accepted Manuscript

This article can be cited before page numbers have been issued, to do this please use: D. Torregrosa, C. Gómez-Pertusa, G. Grindlay, L. Gras and J. Mora, *J. Anal. At. Spectrom.*, 2023, DOI: 10.1039/D2JA00342B.

ROYAL SOCIETY OF CHEMISTRY

rsc.li/jaas

Organics non-spectral interferences on nanoparticle characterization by means single particle inductively coupled plasma mass spectrometry

Daniel Torregrosa, Carlos Gómez-Pertusa, Guillermo Grindlay, Luis Gras, Juan Mora

University of Alicante, Department of Analytical Chemistry, Nutrition and Food Sciences, PO Box 99, 03080 Alicante, Spain.

E-mail: guillermo.grindlay@ua.es

Abstract

The number of works devoted to nanomaterials characterization in organic matrices by means spICP-MS grows every year, but limited information is available about the non-spectral interferences generated by this type of matrices. A better understanding of this interference is a prerequisite for developing more robust methodologies and improving spICP-MS metrology. The goal of this work is to investigate non-spectral interferences due to organics on nanoparticles (NPs) characterization (i.e., number concentration and size distribution) by means spICP-MS. To this end, the influence of NPs composition and size (i.e., Au-, Pt- and SeNPs), carbon source (i.e., 6% w w^{-1} glycerol and 10% w w^{-1} ethanol), ICP-MS operating conditions (i.e., sampling depth and nebulizer gas flow) and instrument design on matrix effects have been evaluated. It was observed that 10% w w^{-1} ethanol give rise to positive matrix effects on the number concentration due to changes on aerosol generation and transport with regard water standards. Irrespective of the organic source

View Article Online
DOI: 10.1039/D2JA00342B

employed, either positive or negative bias on the size distributions can be obtained and these effects depend on plasma operating conditions, instrument characteristics and NPs composition. In addition to changes on transport efficiency, matrix effects on size distribution also depend on plasma characteristics and carbon-based charge transfer reactions (Au and Se). Organic non-spectral interferences can be mitigated by means internal standardization. When operating with 10% w w^{-1} ethanol, two internal standards (ionic solution plus a NPs suspension of known concentration) are simultaneously required for correcting changes on analyte ionization and transport. For 6% w w^{-1} glycerol, however, just a single internal standard (ionic solution) is necessary since this matrix does not affect aerosol generation and analyte transport. A novel measurement procedure is proposed for measuring the internal standards and the NPs of interest without compromising sample throughput.

Keywords: Organics, non-spectral interferences, nanoparticles, single particle, inductively coupled plasma mass spectrometry

View Article Online
DOI: 10.1039/D2JA00342B

1. Introduction

Inductively coupled plasma mass spectrometry operating in single particle mode (spICP-MS) has become a powerful analytical tool for nanomaterials (NMs) characterization in complex samples.[1,2] This technique is based on nebulizing a diluted NMs suspension into the plasma and measuring the time-resolved signal profile generated by nanoparticles ionization. Based on this signal profile, chemical composition, number concentration and size distribution can be obtained for a given NMs suspension. Moreover, the presence of NMs and dissolved forms of specific elements can also be distinguished from spectra signal background.[3]

As in conventional (ionic solution) analysis by means ICP-MS, analytical figures of merit in spICP-MS strongly depend on the occurrence of both spectral and non-spectral interferences generated by sample concomitants and the reagents employed during the sample preparation step. Spectral interferences are generally well-understood and could be mitigated by choosing a non-interfered analyte isotope - if possible - or using a collision/reaction cell.[4,5] As regards non-spectral interferences, they are related to changes in analyte signal by samples concomitants regarding calibration standards.[6] The origin of these interferences is rather complex since concomitants could simultaneously affect: (i) aerosol generation and transport; (ii) plasma characteristics; (iii) analyte ionization mechanisms; and (iv) ion extraction from the plasma to the mass spectrometer. The number of works devoted to study non-spectral interferences with spICP-MS is scarce in contrast with those performed with ICP-MS for ionic solutions. Peters et al.[7] investigated non-spectral interferences for different inorganic (sodium chloride, liver digest and Dulbecco modified Eagle's minimal essential

medium) and organic matrices (methanol and sodium dodecyl sulphate) for a 60 nm Au nanoparticles (NPs) suspension. These authors found that, when operating 1% methanol, 10 mM sodium dodecyl sulphate and 0.05% Dulbecco medium, aerosol generation and transport improved, thus giving rise to a higher number concentration in comparison with water. In addition, an increase in the particle size was observed for the methanol matrix which could be related to carbon-enhancement ionization effect on Au. For 5 g L^{-1} sodium chloride matrix, there was no influence on particle concentration, but size distribution was shifted to lower values due to ionization suppression. No matrix effects on both number concentration and size distribution were reported for the liver digest. Similar findings have been reported by other authors.[8,9] To mitigate the impact of non-spectral interferences on NPs characterization by means spICP-MS, internal standardization and standard addition have been previously proposed.[10,11,12]

So far, fundamental studies about organics non-spectral interferences with spICP-MS have shown a limited scope in terms of matrices (methanol and sodium dodecyl sulphate) and NMs (As-, Ag- and AuNPs) investigated.[7,9] Moreover, the influence of critical instrument parameters on matrix effects (e.g., sampling depth, SD) as well as strategies to mitigate them have not been systematically investigated. The lack of studies in this regard is particularly striking, considering the significant number of applications where organics (or carbon) are present such as petroleum products,[13] enzymatic digestions[14,15,16] and extraction procedures,[17,18] among others. It is therefore obvious that a better understanding of organic non-spectral interferences is a prerequisite for improving method robustness and spICP-MS metrology. The aim of this work is

View Article Online
DOI: 10.1039/D2JA00342B

to systematically investigate organics non-spectral interferences on NPs number concentration and size distributions by means spICP-MS. To this end, the influence of NM composition (i.e., Au-, Pt- and SeNPs) and size, carbon source (i.e., 6% w w^{-1} glycerol and 10% w w^{-1} ethanol), ICP-MS operating conditions (i.e., sampling depth and nebulizer gas flow) and instrument design on matrix effects have been checked. Next, the use of internal standardization for mitigating organic matrix effects on both the number concentration and the number size distribution has been evaluated. Finally, it has been investigated whether organics allow improving number concentration and size limits of detection.

2. Materials and methods

2.1. Reagents

Stock suspensions of citrate-stabilized platinum nanoparticles (PtNPs) with a nominal diameter of 70 nm and a nominal concentration of $1.2 \cdot 10^{10}$ mL^{-1} (NanoComposix, San Diego, USA), sodium dodecyl sulphate-stabilized selenium nanoparticles (SeNPs) with a nominal diameter of 150 nm and a concentration of $2.0 \cdot 10^{10}$ mL^{-1} (Glantreo, Cork, Ireland), and citrate-stabilized gold nanoparticles (AuNPs) with nominal diameters of 50, 100 and 150 nm and concentrations of $3.5 \cdot 10^{10}$, $3.9 \cdot 10^{9}$ and $3.6 \cdot 10^{9}$ mL^{-1} respectively (Cytodiagnostics, Burlington, Canada) were employed through this work.

Gold, Pt and Se mono-elemental 1000 mg L^{-1} standards (Sigma-Aldrich, Schelldorf, Germany) were employed for preparing calibration curves of known mass concentration for spICP-MS size measurements. Arsenic, Ir and Te mono-elemental 1000 mg L^{-1} standards (Sigma-Aldrich, Schelldorf, Germany) were used as internal standards (IS) for mitigating organics non-spectral

interferences on analyte ionization. Finally, 96% w w^{-1} ethanol (Panreac, Barcelona, Spain) and 86-88% w w^{-1} glycerol (Scharlau, Barcelona, Spain) were employed for preparing organic matrix solutions.

2.2. Solutions and suspensions

To evaluate organics non-spectral interferences on both the particle number concentration and size distribution for a given NP, diluted suspensions were prepared by accurately weighing aliquots of the corresponding stock suspension, after 1 min sonication, in: (i) MilliQ water; (ii) 6% w w^{-1} glycerol as a non-volatile carbon source; and (iii) 10% w w^{-1} ethanol as a volatile carbon source. In addition, for each matrix, ionic standards were prepared for calculating NPs size distributions.

For internal standardization, analyte suspensions were spiked with different internal standards for mitigating matrix effects on analyte ionization and transport efficiency. Arsenic, Ir, or Te (10 ng mL^{-1}) were specifically employed to correct changes on analyte ionization (IS_{ion}) whereas Au-, Pt- or SeNPs suspensions ($1 \cdot 10^4$ mL^{-1}) were used to correct changes on transport efficiency (IS_{trans}).

2.3 Instrumentation

Two different quadrupole-based ICP-MS instruments (8900 & 7700x, Agilent, Santa Clara, USA) were employed throughout this work for evaluating carbon non-spectral interferences on NPs characterization by means spICP-MS. These instruments were equipped with the same sample introduction system consisting of a Micromist concentric pneumatic nebulizer and a Scott double pass spray chamber (Agilent, Santa Clara, USA) operating at 2°C. Table 1

View Article Online
DOI: 10.1039/D2JA00342B

gathers operating conditions employed for both instruments.

Unless stated otherwise, data acquisition and analysis were conducted via the single nanoparticle application module present in the software controlling ICP-MS (MassHunter version 4.5). Single particle calibration was carried out using the frequency methodology proposed by Pace et al.[19] Transport efficiency was evaluated using NPs standards of known concentration prepared from stock solutions and elemental dissolved standards were used for building the calibration curve allowing to determine the mass of analyte per NP and hence particle diameter. Because of software constrains for measuring several nuclides sequentially (one-by-one), time-resolved analysis (TRA) mode was employed for implementing internal standardization. In this case, data was manually processed using the RIKILT worksheet operated in Microsoft Excel software.[7] Separation of event signals from background signals was carried out selecting particle detection threshold as 5 times the standard deviation of the baseline (i.e., 5σ criterion).[20]

Prior to ICP-MS measurements, all the NPs were characterized by means transmission electron microscopy (TEM), using a 120 kV JEM-1400 Plus electron microscope (JEOL, Tokio, Japan). Nanoparticle size distribution data afforded by TEM were employed as a reference for optimizing spICP-MS operating conditions and evaluating matrix effects. A detailed description of sample preparation procedure for TEM observations can be found elsewhere.[2]

3. Results and discussion

Gold, Pt- and SeNPs were selected for investigating carbon non-spectral interferences on NMs number concentration and size by spICP-MS. These NMs

View Article Online
DOI: 10.1039/D2JA00342B

are made of hard-to-ionize elements and, hence, organics matrix effects are expected to be significant, particularly due to the occurrence of carbon-based charge transfer reactions.[21] Pure metallic and metalloid NPs were preferred over other NMs (e.g., oxides) due to better suspension stability and narrow size distributions. Considering recent spICP-MS applications[17,18] and the literature about carbon non-spectral interferences with ionic solutions,[21,22,23] 6% w w^{-1} glycerol and 10% w w^{-1} ethanol solutions were selected as organic matrices. These solutions contain the same amount of carbon (i.e., 20 g L^{-1}) and cover different solution physicochemical properties relevant for evaluating organics matrix effects in ICP-MS (Table S1).[21,22,24]

First, spICP-MS operating conditions were optimized for measuring Au-, Pt- and SeNPs suspensions in water. To this end, net analyte pulse intensity was employed.[25] The sample flow rate and r.f. power were, respectively, fixed at 340 µL min^{-1} and 1550 W to favor analyte and matrix atomization/ionization. Consequently, only the influence of the sampling depth and the nebulizer gas flow rate (Q_g) were investigated. For all the analytes, the optimum Q_g was found at 0.9 L min^{-1}. As regards the optimum SD, some differences were noticed between the NPs tested. Thus, the optimum SD for PtNPs and AuNPs (50-150 nm) was 8 mm, but 4 mm was found for SeNPs. Differences in the optimum SD can be explained in terms of analyte boiling point[26] since NPs made of a highly volatile element (i.e., Se 685ºC) requires a smaller path within the plasma to be ionized with regard those made of less volatile element (Au: 2807ºC; and Pt: 3827ºC). No significant influence of analyte ionization energy is expected since all the elements show similar values (Au: 9.23 eV; Pt: 8.95 eV; and Se: 9.75 eV).[26] Under optimum operating conditions for each NPs suspension in water,

View Article Online
DOI: 10.1039/D2JA00342B

the number size distribution obtained by means spICP-MS was equivalent to that afforded by TEM. Nonetheless, the number size distributions for SeNPs were significantly broadened regarding TEM data. Similar observations have been made by Laborda et al.[27] for other type of NMs and can be justified by analyte diffusion within the plasma and overlapping issues between ion clouds generated from different SeNPs due to the low melting point of Se. Next, suspensions of known concentration were prepared with organics (i.e., 6% w w^{-1} glycerol and 10% w w^{-1} ethanol) and analyzed by means spICP-MS using water suspension as a reference.

3.1. Carbon non-spectral interferences for PtNPs

Platinum ionization in ICP-MS is not affected by carbon-based charge transfer reactions in contrast with Au and Se.[21] Therefore, because matrix effects are expected to be less complex, PtNPs were initially selected for assessing carbon non-spectral interferences. No significant changes on both the number of events and $^{195}Pt^{+}$ net signal pulses were noticed for water and 6% w w^{-1} glycerol suspensions (Fig. S1). When operating the ethanol matrix, however, the number of events increased 30% and the average net signal of $^{195}Pt^{+}$ pulses decreased 340% (Fig. S1). Similar differences on $^{195}Pt^{+}$ net signal were observed for ionic solutions in water and ethanol and, hence, it can be rule out that matrix effects are related to incomplete NPs atomization/ionization. Considering these findings, biased results on both the number concentration and the mean particle diameter are expected for 10% w w^{-1} ethanol if no appropriated calibration is performed. For instance, when calibrating with water standards (i.e., PtNPs suspension in water for assessing transport efficiency

View Article Online
DOI: 10.1039/D2JA00342B

and Pt^{+} water standards for calculating mass calibration curve),[19] the number concentration and the mean diameter bias for this matrix were +38% and -67%, respectively (Table 2). In the case of 6% w w^{-1} glycerol, no bias was found and, hence, water standards could be successfully employed for the accurate analysis of PtNPs suspensions in this organic matrix as it has been previously reported for ionic solutions.[21]

To explain results shown in Table 2, it should be considered that organics potentially affect: (i) aerosol generation and transport,[22,24] (ii) discharge characteristics (e.g., plasma temperature),[22,28] and (iii) atomization/ionization mechanisms.[21,29,30,31] As it has been previously mentioned, Pt ionization is not affected by carbon-based charge transfer reaction[21] and hence, only the two first phenomena are relevant to explain experimental data. Our research group has previously demonstrated that aerosol generation and transport as well as plasma thermal conditions for diluted nitric acid and 6% w w^{-1} glycerol are similar.[29] This means that no significant differences on the number concentration and the number size distribution should be expected for both matrices. 10% w w^{-1} ethanol solutions show, however, a lower surface tension and higher volatility than water thus improving aerosol transport to the plasma (Table S1).[24] This leads to an increase in the number of events but negatively affects plasma thermal properties due to the excess of energy required to deal with the higher solvent load. While plasma temperature has not been specifically assessed, it was observed that the optimum Q_g for the analysis of PtNPs and Pt ionic solutions in 10% w w^{-1} ethanol (i.e., 0.8 L min^{-1}) was lower than with water and 6% w w^{-1} glycerol (i.e., 0.9 L min^{-1}). These results suggest that the former matrix deteriorates discharge characteristics and, hence, Q_g

View Article Online
DOI: 10.1039/D2JA00342B

should be decreased to favor matrix decomposition and analyte ionization. Plasma cooling effects by ethanol decrease Pt ionization and, hence, the apparent mean diameter for this matrix was smaller than for water. According to this, carbon matrix effects for organics should be more significant at plasma base, and they should decline when increasing SD. To confirm this hypothesis, NPs size distributions for all the matrices were obtained below (4 mm) and above (12 mm) the optimum SD (Fig. 1). As expected, matrix effects for ethanol were higher at 4 mm and decreased with SD. Nevertheless, even at a SD of 12 mm, the number size distribution for PtNPs was still biased -20%. On the other hand, it was observed that PtNPs size distribution in glycerol was also biased (-10%) at 4 mm thus confirming that discharge temperature is negatively affected even for non-volatile organics at plasma base. It is important to note that, for all the matrices tested, particle size distributions are significantly broadened at 4 mm with regard higher SD and TEM data. This broadening can be justified with the occurrence of different phenomena (i.e., aerosol size distribution heterogeneity, radial distribution of particles in the plasma and partial pulse measurements) which are expected to affect signal pulses intensity more significantly at low SD where solvent vaporization and atomization is not fully accomplished.[27] Finally, within experimental uncertainties, there was no influence of SD on the number of events for water and 10% w w^{-1} ethanol. Consequently, signal bias on the number concentration operating 10% w w^{-1} ethanol was constant with SD. These results are expected since, unless the discharge is severely deteriorated, pulse frequency mainly depends on aerosol transport efficiency.

3.2. Carbon non-spectral interferences for SeNPs

Because Se ionization is specifically affected by carbon-based charge transfer reactions, matrix effects for SeNPs are expected to be different to those previously shown by PtNPs. Unexpectedly, under optimum experimental conditions for water suspension introduction (Q_g 0.9 L min^{-1}, SD 4 mm), the appearance of $^{78}Se^+$ time scans for SeNPs suspensions (Fig. S2) looked like those obtained for PtNPs (Fig. S1). That is, there was no difference on signal spectra between water and 6 % w w^{-1} glycerol suspensions, but the number of events increased, and signal pulses were reduced for 10% w w^{-1} ethanol suspension. Consequently, the number concentration, the mean diameter and the size distribution for SeNPs in the latter matrix were significantly biased operating water calibration standards (Table 2 and Fig. 2.A). It is important to remark that matrix effects on SeNPs number concentration with 10% w w^{-1} ethanol were equivalent to those early found for PtNPs, thus indicating that transport changes by ethanol are similar for both type of NPs.

According to the above-mentioned findings, carbon non-spectral interferences for SeNPs in 10% w w^{-1} ethanol were only related to changes on aerosol phenomena and plasma characteristics. Carbon charge transfer reactions did not seem to play a significant role, probably since carbon ionization was not significant at plasma base (4 mm) by organics plasma cooling effects. Therefore, carbon non-spectral matrix effects were also examined at higher SD (8 mm, Fig. 2.B; and 12 mm, Fig. 2.C) where C^+ levels are expected to be higher. When operating 6% w w^{-1} glycerol, $^{78}Se^+$ signal was indeed improved with regard water at 8 mm and 12 mm (Fig. S3 and S4). Consequently, the number size distribution for this matrix was significantly biased to larger

View Article Online
DOI: 10.1039/D2JA00342B

diameters. For instance, mean diameter bias at 8 and 12 mm was, respectively, +42 and +43%. According to these data, carbon-based charge transfer reactions were only relevant at higher SD. This phenomenon was also present for 10% w w^{-1} ethanol and counterbalanced plasma thermal degradation effects (Fig. S3 and S4). In fact, the number size distribution bias between 10% w w^{-1} ethanol and water could be even positive at 12 mm (+9%). Finally, as it has already been mentioned in Section 3.1, matrix effects on the number concentration for 10% w w^{-1} ethanol were independent of SD.

3.3. Carbon non-spectral interferences for AuNPs

Gold NPs ranging from 50 to 150 nm were selected to investigate carbon non-spectral interferences. Since this element is affected by carbon-based charge transfer reactions, it is feasible to evaluate whether this phenomenon depends on NPs dimensions.[10] Under optimum experimental conditions for AuNPs (Q_g 0.9 L min^{-1}, SD 8 mm), $^{197}Au^+$ signal spectra differ to that shown for PtNPs due to the occurrence of carbon-based charge transfer reactions. Thus, the average $^{197}Au^+$ signal pulse mean for the 6% w w^{-1} glycerol suspension was enhanced 1.6 times with regards the water suspension. On the other hand, $^{197}Au^+$ signal pulse suppression by 10% w w^{-1} ethanol was less significant than the values observed for PtNPs under similar experimental conditions (Fig. S5-S7). According to these findings, mean particle diameter was biased to larger values for 6% w w^{-1} glycerol whereas carbon matrix effects for 10% w w^{-1} ethanol were reduced (Fig. S8-S10). Carbon matrix effects on number size distributions were similar for all the AuNPs tested and, within experimental errors, they are independent of NPs size at least up to 150 nm (Table 2). Finally, peak

View Article Online
DOI: 10.1039/D2JA00342B

broadening effects and carbon non-spectral interferences on the number particle concentration were equivalent to those explained before for PtNPs.

3.4. Influence of instrument design on carbon non-spectral interferences

Several reports have shown that carbon matrix effects in ICP-based techniques are not solely dependent on aerosol generation and transport, plasma characteristics and ionization mechanisms but also on instrument design (e.g., r.f. generator, torch design, etc.).[10,28,32] For this reason, carbon non-spectral matrix effects were also investigated using an alternative quadrupole-based ICP-MS instrument (Agilent 7700x) equipped with the same sample introduction employed in previous experiments (i.e., Micromist nebulizer coupled to a Scott double pass spray chamber). Because no changes are introduced into sample introduction system, differences on matrix effects between both instruments (Agilent 8900 and 7700x) should reflect other factors influencing carbon non-spectral interferences.

Optimum experimental conditions for NPs analysis in water suspension by means 7700x ICP-MS model were different to those outlined before for 8900 one. Irrespective of NPs characteristics, optimum Q_g and SD were, respectively, 1.1 L min^{-1} and 4 mm. Since the ionization for all the NPs takes place closer to plasma base (i.e., no influence of NPs composition), these results suggest that the Agilent 7700x model is apparently more robust than the 8900 one. As expected from previous findings, when calibrating with water standards, the number concentration for all the NPs with the Agilent 7700x model was biased operating 10% w w^{-1} ethanol but not 6% w w^{-1} glycerol (Table 3). Number concentration skew for 10% w w^{-1} ethanol suspension was similar for all the

View Article Online
DOI: 10.1039/D2JA00342B

NPs investigated and it was on average +50%. This bias was higher than that observed with 8900 ICP-MS, probably because the former instrument operates at higher Q_g (1.1 L min^{-1} vs 0.9 L min^{-1}) which proportionally favors solvent evaporation and aerosol transport.

On the other hand, the mean particle diameter (Table 3) and the particle size distribution (Fig. 3) for all the NPs operating organics were shifted to larger diameters regarding the water suspension. Positive matrix effects for PtNPs size distributions with organics were totally unexpected considering that this element is not affected by carbon charge-transfer reactions.[21] Nevertheless, it was observed that plasma was slightly contracted operating organics thus giving rise to a more energetic discharge (thermal pinch effect)[28] which favors Pt ionization (i.e., higher Pt pulses). According to this argument, carbon-based charge transfer reactions are also favored (i.e., higher carbon ionization) and, hence, matrix effects for Au- and SeNPs are higher than those observed before with 8900 ICP-MS (Table 2, Fig. 1 and 2, Fig. S8-S10).

3.5. Carbon non-spectral interferences correction

To correct carbon non-spectral interferences for real sample analysis, different calibration strategies are feasible. Matrix-matched standard calibration is the most straightforward approach, but it is difficult to be applied in routine analysis. Aramendía et al.[12] have recently proposed the use of standard addition for addressing non-spectral interferences in spICPMS. This strategy successfully corrects both inorganic and organic-based non-spectral interferences. Nevertheless, this approach is less advantageous in terms of sample throughput since several standards should be analyzed for each sample analyzed and it could be challenging to apply when the number concentration

View Article Online
DOI: 10.1039/D2JA00342B

levels are high (e.g., double events). Alternatively, internal standardization can be employed. This approach only requires sample spiking with a known concentration of species originally not present in the sample but at the expense of decreasing sample throughput due to the limited multi-element monitoring capabilities afforded by quadrupole instruments. So far, this calibration strategy has been successfully employed for mitigating saline matrix effects.[10,11] However, no previous attempts to specifically correct matrix effects for organics matrices have been reported.

As already explained, organic non-spectral interferences on the number concentration and size distribution for 6% w w^{-1} glycerol and 10% w w^{-1} ethanol are based on different phenomena (i.e., aerosol generation and transport, plasma characteristics and carbon-based charge transfer reactions) and, hence, the appropriate selection of an IS for mitigating matrix effects is not a trivial task. For 6% w w^{-1} glycerol, because there are no changes on transport efficiency with regard water standards, matrix effects could be corrected using a single IS that behaves similarly to the analyte of interest. The picture is different for 10% w w^{-1} ethanol since this matrix improves NPs transport efficiency, but ionic signals could be either enhanced or suppressed. In fact, when positive matrix effects are observed, changes on aerosol transport and ionic signals behave differently. So, a single standard cannot be simultaneously employed for addressing non-spectral interferences on the number concentration and the size distribution for this matrix. According to this argument, different ISs have been investigated for addressing matrix effects on analyte ionization (IS_{ion}) and transport efficiency (IS_{trans}). The following nuclides were investigated as IS_{ion}: $^{75}As^{+}$, $^{125}Te^{+}$ and $^{193}Ir^{+}$. These species cover different physicochemical

View Article Online
DOI: 10.1039/D2JA00342B

properties which might affect correction accuracy (e.g., ionization energy, m/z changes on analyte ionization by carbon-based charge transfer reactions). On the other hand, Au-, Pt- and SeNPs suspensions of known concentration were tested as IS_{trans} for mitigating changes on transport efficiency. *A priori*, all the above-mentioned suspensions could be indistinctively employed as IS_{trans} since matrix effects on aerosol transport by 10% w w^{-1} ethanol are similar.

In order to apply internal standardization without compromising sample throughput for quadrupole ICP-MS instruments, we have devised a measurement protocol to maximize instrument data acquisition by mimicking the calibration strategy employed for isotope ratio measurements.[33] Since a significant fraction of time is lost when measuring several nuclides simultaneously during acquisition time, ICP-MS was configured to measure them sequentially (one-by-one) using a bracketing approach as follows (Fig. 4): (i) IS_{ion} (15 s); (ii) IS_{trans} (30 s); (iii) sample (60 s); (iv) IS_{trans} (30 s); and (v) IS_{ion} (15 s). This protocol specifically requires the use of software transient signal mode (TRA) since it allows for measuring several nuclides sequentially and independently. Operating this way, the analysis of a given sample only takes 150 s which is faster than previous approaches based on the use of a single IS (180-400 s)[10,11] as well as on standard addition (180-360 s, depending on the number of ionic standards employed).[12] The main drawback of this approach is that experimental data should be processed externally thus increasing time for data treatment but it could be easily solved by updating instrument software. It is important to highlight the analysis time could be even further reduced. Because software constrains, TRS mode stablishes a minimum of 15 seconds for measuring each nuclide, but 5 seconds was usually enough for measuring a

representative ionic signal (steps i and v). Nanoparticle mean diameter and number concentration operating organics for Agilent 7700x instrument with and without internal standardization are gathered in Tables 4 and 5, respectively. Internal standardization was applied using each IS individually (IS_{ion} or IS_{trans}) and combined (IS_{ion} + IS_{trans}).

In agreement with previous studies,[10,11] IS_{ion} was useful to mitigate carbon matrix effects on Au- SeNPs size distributions for 6% w w^{-1} glycerol. By the appropriate selection of the IS_{ion}, size diameter bias was always lower than 5%, thus indicating that no matrix effects were detectable (t-test at a 95% confidence level). Since both As and Te ionization are affected by carbon-based charge transfer reactions, these species are suitable internal standard for mitigating carbon matrix effects for SeNPs in 6% w w^{-1} glycerol (Tables 4 and S2). *A priori*, As and Te should have been good IS_{ion} for AuNPs, but better results were obtained for Ir. It must be considered that, unlike Au, As and Te ionization is particularly sensitive to carbon-based charge transfer and, hence, size distributions were overcorrected with these species. As regards PtNPs in 6% w w^{-1} glycerol, there was no benefit of using IS_{ion} (Ir) given that this matrix does not lead to significant non-spectral interferences on Pt ionization. Because transport efficiency for both water and 6% w w^{-1} glycerol are equivalent, IS_{trans} (or IS_{ion} + IS_{trans}) is not required for correcting number concentration data (Tables 5 and S3), regardless the instrument used. This means that the measuring protocol can be shortened to 90 s by eliminating IS_{trans} measurement time (steps ii and iv). When operating 10% w w^{-1} ethanol, however, carbon matrix effects correction was trickier than with 6% w w^{-1} glycerol. The former matrix affects aerosol transport and, hence, matrix effects on the number

concentration are only addressed by using IS_{trans} (Tables 5 and S3). No significant influence of the NPs suspension employed as IS_{trans} (Au-, Pt- or SeNPs) for correcting matrix effects was noticed. Therefore, all the NPs tested in this work could be indistinctively employed as IS_{trans}. Obviously, because IS_{trans} does not correct changes on analyte ionization, it can not be employed for addressing matrix effects on NPs mean diameter. To this end, the use of an IS_{ion} is mandatory. There were no significant differences on PtNPs and AuNPs mean diameter between this matrix and the reference using Ir as IS_{ion} but biased results (-10/-20%) were obtained for SeNPs regardless the IS_{ion} employed (As or Te) (Tables 4 and S2). Only a combination of ISs (IS_{ion} + IS_{trans}) allows mitigating matrix effects on SeNPs mean size. Similar conclusions to those outlined above for Agilent 7700x ICP-MS were noticed for Agilent 8900 model (Tables S2 and S3).

3.6. Influence of organics on the number concentration and size limit of detection.

Considering that both aerosol transport and analyte ionization might be enhanced under certain operating conditions by organics, it has been investigated whether organics improve spICP-MS detection capabilities regarding water. For all the NPs, number concentration (LOD_{Conc}) and size limits of detection (LOD_{Size}) were measured under optimum operating conditions for each matrix with both Agilent 8900 and 7700x ICP-MS instruments.

3.6.1. Number concentration limit of detection

Number concentration limit of detection was estimated according to the following equation, based on the work of Laborda et al:[34]

View Article Online
DOI: 10.1039/D2JA00342B

$$LOD_{Conc} = \frac{5 \cdot \sigma_{N,B} + 3}{\eta_n \cdot Q_l \cdot t_{Scan}} \quad (1)$$

where $\sigma_{N,B}$ is the standard deviation of the number of particles detected in at least 10 replicate measurements of the blank; η_N, transport efficiency; Q_l, sample uptake rate (mL min^{-1}); and t_{Scan}, measuring time (min). In the particular case that no NPs are detected in the blank, Equation 1 can be simplified as follows:[34]

$$LOD_{Conc} = \frac{3}{\eta_n \cdot Q_l \cdot t_{Scan}} \quad (2)$$

Given that blanks in this study were only the solvents solutions and no particles were detected in any of them, Equation 2 was preferred to stablish LOD_{Conc}.

Table 6 gathers LOD_{Conc} for all the NPs in water and organics operating Agilent 7700x ICP-MS. As expected from differences on aerosol generation and transport, LOD_{Conc} was improved on average 50% for the ethanol matrix but there was no difference between water and glycerol. According to Equation 2, any improvement on transport efficiency affects directly LOD_{Conc}. Therefore, unless plasma conditions are severely deteriorated, the better the aerosol generation and transport the better LOD_{Conc} is achieved. Similar conclusions were found with 8900 ICP-MS.

3.6.2. Size limit of detection

Size limit of detection was estimated using the following equation:[3]

$$LOD_{Size} = 10^{4.3} \sqrt{\frac{6 \cdot L \cdot t_{Dwell} \cdot Q_l \cdot \eta_n \cdot f_a}{\pi \cdot \rho_{NP} \cdot b_{Cal} \cdot 60}} \quad (3)$$

where L is the particle detection threshold (i.e., 5σ criterion) (counts); t_{Dwell}, dwell time (s); f_a, fraction of analyte in the NP; ρ_{NP}, nanoparticle density (g mL^{-}

^{1}); and b_{Cal}, ICP-MS response for ion standard (counts mL ng^{-1}). Size limits of detection obtained for Agilent 7700x are gathered on Table 6.

Because organics do not significantly affect analyte ionization and background noise, Pt- and AuNPs LOD_{Size} were independent of the matrix considered. For SeNPs, however, LOD_{Size} afforded by organic matrices were slightly lower than those obtained with water due to the beneficial effect of carbon-based charge transfer reactions on analyte ionization. Though organics favor Se ionization, LOD_{Size} improvement is limited due to changes on sensitivity are damped due to the cubic root present in Equation 3. Selenium sensitivity in 10 w w^{-1} % ethanol was 2 times higher than in water which was equivalent to a 1.25-fold improvement in LOD_{Size}. Similar conclusions to those outlined above were found with 8900 ICP-MS. In fact, since this instrument is less robust, no improvement on LOD_{Size} for SeNPs was noticed operating organics.

4. Conclusions

From the results obtained in the present work it can be concluded that carbon non-spectral interferences in spICP-MS are complex and depend on: (i) sample physicochemical properties. Volatile organics favors aerosol generation and transport thus giving rise to higher analyte transport efficiency (i.e., higher number concentration); (ii) plasma operating conditions and instrument design. Because the atomization of organics requires more energy than water, matrix effects on the number size distributions strongly depend on sampling depth. In fact, either positive or negative bias can be obtained depending on plasma robustness and changes on analyte ionization due to carbon-based charge transfer reactions; and (iii) NMs composition. Though Au and Se ionization is

View Article Online
DOI: 10.1039/D2JA00342B

affected by carbon, number size distribution bias for SeNPs was higher than for AuNPs under a given set of experimental conditions.

Internal standardization allows mitigating carbon non-spectral interferences. For non-volatile organics, matrix effects on analyte ionization could be mitigated using a single IS (i.e., ionic solution). However, when operating volatile solvents, a second IS for addressing matrix effects on transport efficiency is mandatory. To this end, the sample of interest should be spiked with a NPs suspension of known concentration. By the appropriate selection of the measuring conditions, it is feasible to measure the sample and both ISs without compromising sample throughput.

Organics are widely employed as an additive in ICP-MS for improving analytical figures of merit due to beneficial effect on transport efficiency and analyte ionization for ionic solutions. According to our data, the benefits afforded by organics with spICP-MS are more limited. While volatile solvents improve number concentration detection limits, the effect of organics on size detection limits are less significant, even for NMs made of elements involved in carbon-based charge transfer reactions (e.g., Se and Au).

Acknowledgements

The authors would like to thank the Generalitat Valenciana (PROMETEO/2021/055) and the Vice-Presidency for Research and Knowledge Transfer of the University of Alicante for the financial support of this work (VIGROB-050). D. Torregrosa thanks the Spanish Ministerio de Ciencia, Innovación y Universidades for the fellowship FPU17/02853.

View Article Online
DOI: 10.1039/D2JA00342B

Table 1. spICP-MS operating conditions.

	Agilent 8900	Agilent 7700x
Plasma forward power (w)	1550	
Sampling depth (mm)	4-12	
Sampling torch injector ID (mm)	0.8	1.2
Argon flow rate (L min^{-1})		
Plasma	15	
Auxiliary	0.9	
Nebulizer	0.8/0.9	1.1
Sample introduction system		
Nebulizer	Micromist	
Spray chamber	Scott double pass	
Sample uptake rate (µL min^{-1})	340	
Dwell time (ms)	0.1	10
Measuring time (s)	60-150	60-150

Table 2. Number concentration and mean particle diameter for Au-, Pt- and SeNPs in different matrices operating water calibration standards with Agilent 8900 ICP-MS. AuNPs and PtNPs operating conditions: Q_g 0.9 L min^{-1}; SD 8 mm. SeNPs: Q_g 0.9 L min^{-1}; SD 4 mm.

	Concentration (10^4 mL^{-1}) (Bias)					Mean diameter (nm) (Bias)				
NP element	**Pt**	**Se**	**Au**			**Pt**	**Se**	**Au**		
Nominal size (nm)	**70**	**150**	**50**	**100**	**150**	**70**	**150**	**50**	**100**	**150**
Sample										
Reference	1.3 ± 0.2	2.0 ± 0.2	2.5 ± 0.3	3.5 ± 0.4	2.1 ± 0.2	71 ± 4	154 ± 12	52 ± 4	102 ± 8	155 ± 12
Water	1.3 ± 0.3	2.0 ± 0.2	2.8 ± 0.3	3.7 ± 0.2	2.3 ± 0.2	70 ± 2	153 ± 2	49 ± 3	103 ± 2	150 ± 2
6% w w^{-1} Glycerol	1.2 ± 0.3	1.7 ± 0.4	2.3 ± 0.3	3.3 ± 0.3	2.0 ± 0.2	74 ± 2	156 ± 2	58 ± 2 (+10%)	116 ± 2 (+12%)	168 ± 3 (+9%)
10% w w^{-1} Ethanol	1.8 ± 0.2 (+38%)	2.8 ± 0.4 (+40%)	3.4 ± 0.6 (+36%)	4.7 ± 0.4 (+34%)	2.8 ± 0.2 (+33%)	47 ± 2 (-67%)	107 ±2 (-70%)	32 ± 2 (-38%)	65 ± 2 (-37%)	103 ± 2 (-32%)

Table 3. Number concentration and mean particle diameter for Au-, Pt- and SeNPs in different matrices operating water calibration standards with Agilent 7700x ICP-MS. AuNPs, PtNPs, and SeNPs operating conditions: Q_g 1.1 L min^{-1}; SD 4 mm.

	Concentration (10^4 mL^{-1}) (Bias)					Mean diameter (nm) (Bias)				
NP element	**Pt**	**Se**	**Au**			**Pt**	**Se**	**Au**		
Nominal size (nm)	**70**	**150**	**50**	**100**	**150**	**70**	**150**	**50**	**100**	**150**
Sample										
Reference	1.3 ± 0.7	2.0 ± 0.2	1.5 ± 0.2	2.0 ± 0.2	1.0 ± 0.2	71 ± 4	154 ± 12	52 ± 6	102 ± 8	155 ± 12
Water	1.4 ± 0.4	2.1 ± 0.2	1.8 ± 0.3	2.1 ± 0.3	1.2 ± 0.2	71 ± 2	153 ± 4	49 ± 2	99 ± 2	149 ± 2
6% w w^{-1} Glycerol	1.6 ± 0.6	2.0 ± 0.1	1.6 ± 0.2	2.2 ± 0.2	1.2 ± 0.2	75 ± 3	237 ± 2 (+55%)	59 ± 2 (+19%)	114 ± 2 (+15%)	172 ± 2 (+15%)
10% w w^{-1} Ethanol	2.1 ± 0.2 (+62%)	3.4 ± 0.2 (+61%)	3.0 ± 0.3 (+61%)	3.2 ± 0.2 (+60%)	1.6 ± 0.2 (+60%)	74 ± 2	237 ± 2 (+55%)	56 ± 2 (+14%)	109 ± 2 (+10%)	166 ± 2 (+11%)

Table 4. Nanoparticle mean diameter oeprating organic matrices with and without internal standardization. Calibration: water standards. Instrument: Agilent 7700x. AuNPs, PtNPs, and SeNPs operating conditions: Q_g 1.1 L min^{-1}; SD 4 mm.

	Mean diameter (nm)									
Matrix	**6% w w^{-1} glycerol**					**10% w w^{-1} ethanol**				
NP element	**Pt**	**Se**		**Au**		**Pt**	**Se**		**Au**	
Nominal size (nm)	**70**	**150**		**50**	**100**	**150**	**70**	**150**		**50**	**100**	**150**
Sample												
Reference	71 ± 4	154 ± 12		52 ± 6	102 ± 8	155 ± 12	71 ± 4	154 ± 12		52 ± 6	102 ± 8	155 ± 12
No IS	69 ± 3	237 ± 9		59 ± 2	114 ± 5	172 ± 7	60 ± 2	237 ± 9		56 ± 2	109 ± 4	166 ± 7
IS_{ion} correction (IS_{ion})	73 ± 3 (Ir)	149 ± 6 (As)	147 ± 6 (Te)	51 ± 2 (Ir)	105 ± 4 (Ir)	157 ± 6 (Ir)	68 ± 3 (Ir)	138 ± 6 (As)	127 ± 5 (Te)	50 ± 2 (Ir)	102 ± 4 (Ir)	153 ± 6 (Ir)
IS_{trans} correction (IS_{trans})	69 ± 3 (AuNPs)	237 ± 9 (PtNPs)		59 ± 2 (PtNPs)	114 ± 5 (PtNPs)	172 ± 7 (PtNPs)	85 ± 2 (AuNPs)	279 ± 2 (PtNPs)		63 ± 2 (PtNPs)	122 ± 3 (PtNPs)	184 ± 3 (PtNPs)
IS_{ion} + IS_{trans} correction (IS_{ion}/IS_{trans})	73 ± 3 (Ir/AuNPs)	149 ± 6 (As/PtNPs)	147 ± 6 (Te/PtNPs)	51 ± 2 (Ir/PtNPs)	105 ± 4 (Ir/PtNPs)	157 ± 6 (Ir/PtNPs)	74 ± 3 (Ir/AuNPs)	154 ± 6 (As/PtNPs)	146 ± 6 (Te/PtNPs)	58 ± 2 (Ir/PtNPs)	110 ± 5 (Ir/PtNPs)	165 ± 7 (Ir/PtNPs)

Table 5. Nanoparticle number concentration operating organic matrices with and without internal standardization. Calibration: water standards. Instrument: Agilent 7700x. AuNPs, PtNPs, and SeNPs operating conditions: Q_g 1.1 L min^{-1}; SD 4 mm.

	Concentration (10^4 mL^{-1})									
Matrix	**6% w w^{-1} glycerol**					**10% w w^{-1} ethanol**				
NP element	**Pt**	**Se**	**Au**			**Pt**	**Se**	**Au**		
Nominal size (nm)	**70**	**150**	**50**	**100**	**150**	**70**	**150**	**50**	**100**	**150**
Sample										
Reference	1.3 ± 0.7	2.0 ± 0.2	1.5 ± 0.2	2.0 ± 0.2	1.0 ± 0.2	1.3 ± 0.7	2.0 ± 0.2	1.5 ± 0.2	2.0 ± 0.2	1.0 ± 0.2
No IS	1.6 ± 0.6	2.0 ± 0.1	1.6 ± 0.2	2.2 ± 0.2	1.2 ± 0.2	2.1 ± 0.2	3.4 ± 0.2	3.0 ± 0.3	3.2 ± 0.2	1.6 ± 0.2
IS_{trans} correction (IS_{trans})	1.6 ± 0.6 (AuNPs)	2.0 ± 0.1 (PtNPs)	1.6 ± 0.2 (PtNPs)	2.2 ± 0.2 (PtNPs)	1.2 ± 0.2 (PtNPs)	1.1 ± 0.2 (AuNPs)	1.9 ± 0.2 (PtNPs)	1.8 ± 0.3 (PtNPs)	2.3 ± 0.2 (PtNPs)	1.2 ± 0.3 (PtNPs)

Table 6. Number concentration and size limit of detection for Au-, Pt- and SeNPs with water and organics. Measuring conditions: Q_g 1.1 L min^{-1}; SD 4 mm. Instrument: Agilent 7700x ICP-MS.

	LoD_{Conc} (particles mL^{-1})			LoD_{Size} (nm)		
Matrix	**Water**	**6% w w^{-1} Glycerol**	**10% w w^{-1} Ethanol**	**Water**	**6% w w^{-1} Glycerol**	**10% w w^{-1} Ethanol**
NP element						
Pt	130	130	90	27	23	32
Se	220	220	130	100	80	80
Au	170	170	120	21	18	19

View Article Online
DOI: 10.1039/D2JA00342B

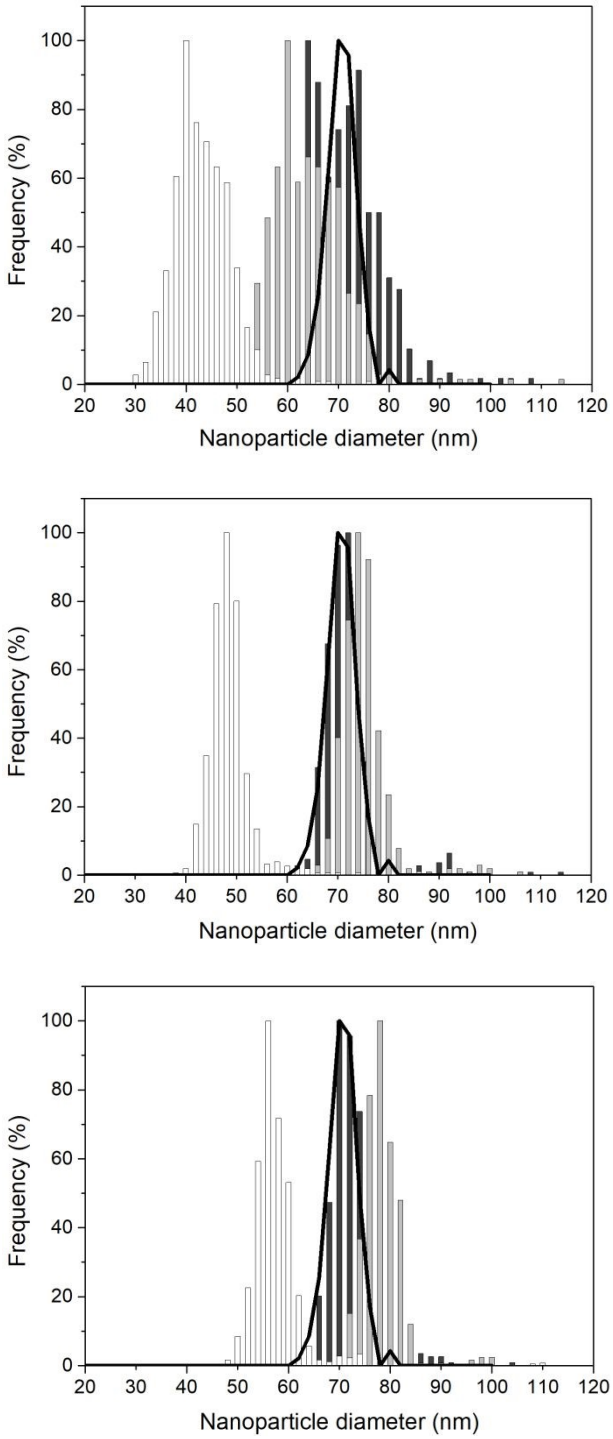

Figure 1. Influence of matrix composition on 70 nm PtNPs size distribution at SD position of (A) 4 mm; (B) 8 mm; and (C) 12 mm for all the matrices investigated. Matrices: water (dark grey bars); 6% w w^{-1} glycerol (light grey bars); and 10% w w^{-1} ethanol (white bars). Size distribution by means TEM is highlighted with a black line. Number concentration of PtNPs: $1.3 \cdot 10^4$ mL^{-1}. Instrument: Agilent 8900 ICP-MS. Calibration: water standards.

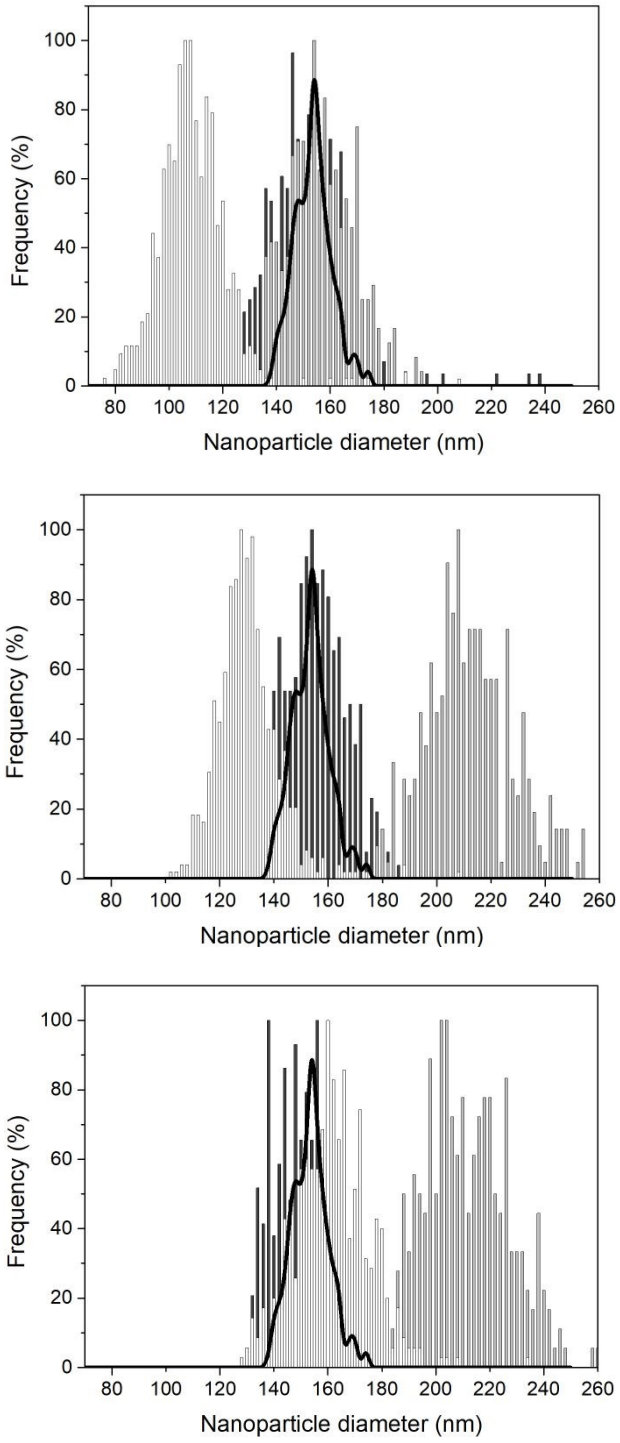

Figure 2. Influence of matrix composition on 150 nm SeNPs size distribution at sampling depth position of (A) 4 mm; (B) 8 mm; and (C) 12 mm. Matrices: water (dark grey bars); 6% w w^{-1} glycerol (light grey bars); and 10% w w^{-1} ethanol (white bars). Size distribution by means TEM is highlighted in a black line. Number concentration of SeNPs: $2.0 \cdot 10^4$ mL^{-1}. Instrument: Agilent 8900 ICP-MS. Calibration: water standards.

View Article Online
DOI: 10.1039/D2JA00342B

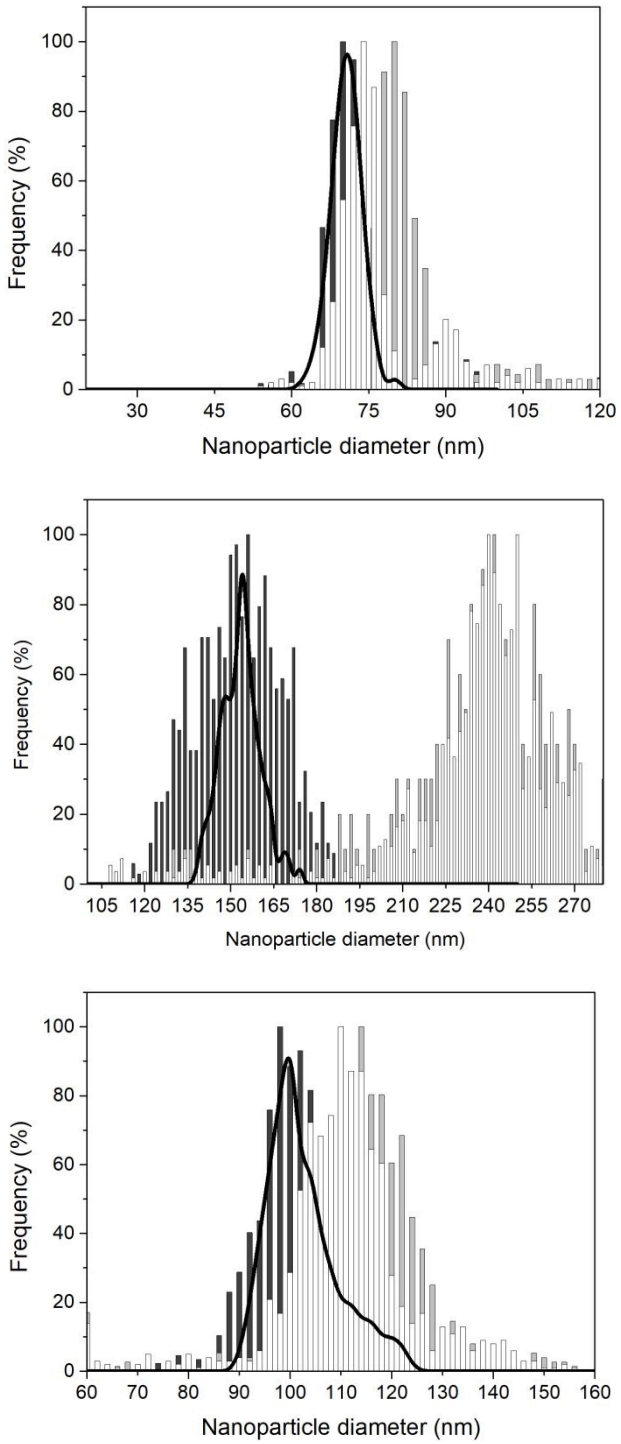

Figure 3. Influence of matrix composition on (A) 70 nm PtNPs; (B) 150 nm SeNPs; and (C) 100 nm AuNP size distributions. Matrices: water (dark grey bars); 6% w w^{-1} glycerol (light grey bars); and 10% w w^{-1} ethanol (white bars). Size distribution by means TEM is highlighted in a black line. Number concentration of PtNPs: $7.0 \cdot 10^3$ mL^{-1}. Number concentration of SeNPs: $2.0 \cdot 10^4$ mL^{-1}. Instrument: Agilent 7700x ICP-MS. Calibration: water standards.

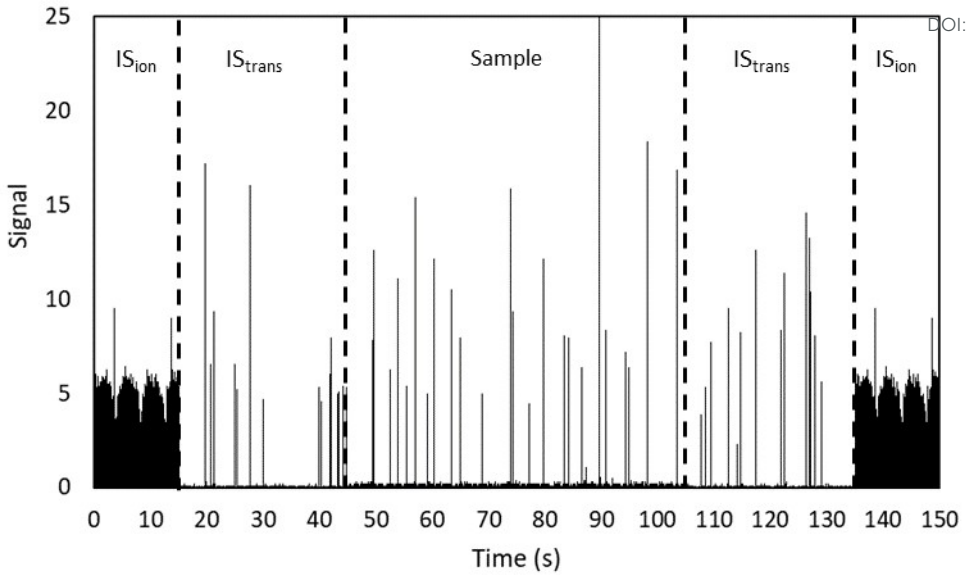

Figure 4. Sample and internal standardization measuring protocol for correcting changes on both analyte ionization and NPs transport (IS_{ion} & IS_{trans}).

View Article Online
DOI: 10.1039/D2JA00342B

References

1 D. Mozhayeva and C. Engelhard, *J. Anal. At. Spectrom.*, 2020, **35**, 1740.

2 D. Torregrosa, G. Grindlay, M. de la Guardia, L. Gras and J. Mora, *Talanta*, 2023, **252**, 123818.

3 F. Laborda, E. Bolea and J. Jiménez-Lamana, *Anal. Chem.*, 2014, **86**, 2270.

4 I. Kálomista, A. Kéri and G. Galbács, *J. Anal. At. Spectrom.*, 2016, **31**, 1112.

5 E. Bolea-Fernández, D. Leite, A. Rua-Ibarz, T. Liu, G. Woods, M. Aramendía, M. Resano and F. Vanhaecke, *Anal. Chim. Acta*, 2019, **1077**, 95.

6 C. Agatemor and D. Beauchemin, *Anal. Chim. Acta*, 2011, **706**, 66.

7 R. Peters, Z. Herrera-Rivera, A. Undas, M. van der Lee, H. Marvin, H. Bouwmeester and S. Weigel. *J. Anal. At. Spectrom.*, 2015, **30**, 1274.

8 M. Witzler, F. Kullmer and K. Gunther, *Anal. Lett.*, 2018, **51**, 587.

9 M. Loula, A. Kana and O. Mestek, Talanta, 2019, **202**, 565.

10 Y. Huang, J. Tsz-Shan Lum and K.S.Y. Leung, *J. Anal. At. Spectrom.*, 2020, **35**, 2148.

11 H. El Hadri, E.J. Petersen and M.R. Winchester, *Anal. Bioanal. Chem.*, 2016, **408**, 5099.

12 M. Aramendía, J.C. García-Mesa, E. Vereda Alonso, R. Garde, A. Bazo, J. Resano and M. Resano, *Anal. Chim. Acta,* 2022, **1205**, 339738.

13 D. Ruhland, K. Nwoko, M. Perez and J.Feldmann, E. M. Krup, *Anal. Chem.* 2019, **91**, 1164.

14 R.J.B. Peters, Z. Herrera Rivera, G. van Bemmel, H.J.P. Marvin, S. Weigel and H. Bouwmeester, *Anal. Bioanal. Chem.,* 2014, **406**, 3875.

15 J. Jiménez-Lamana, I. Abad-Álvaro, K. Bierla, F. Laborda, J. Szpunar and R.

View Article Online
DOI: 10.1039/D2JA00342B

Lobinski, *J. Anal. At. Spectrom.,* 2018, **33**, 452.

16 J.J. López-Mayán, S. del-Ángel-Monroy, E. Peña-Vázquez, M.C. Barciela-Alonso, P. Bermejo-Barrera and A. Moreda-Piñeiro, *Talanta*, 2022, **236**, 122856.

17 L. Torrent, F. Laborda, E. Marguí, M. Hidalgo and M. Iglesias, *Anal. Bioanal. Chem.* 2019, **411**, 5317.

18 J. López-Mayan, M.C. Barciela-Alonso, M. R. Domínguez-González, E. Peña-Vázquez and P. Bermejo-Barrera, *Microchem. Journal*, 2020, **152**, 104264.

19 H.E. Pace, N.J. Rogers, C. Jarolimek, V.A. Coleman, C.P. Higgins and J. F. Ranville, *Anal. Chem.,* 2011, **83**, 9361.

20 J. Tuoriniemi, G. Cornelis and M. Hassellöv, *Anal. Chem.*, 2012, **84**, 3965.

21 G. Grindlay, J. Mora, M.T.C. de Loos-Vollebregt and F. Vanhaecke, *Spectrochim. Acta B*, 2013, **86**, 42.

22 A. Leclerq, A. Nonell, J.L. Todolí, C. Bresson, L. Vio, T. Vercouter and F. Chartier, *Anal. Chim. Acta*, 2015, **885**, 33.

23 A. Leclerq, A. Nonell, J.L. Todolí, C. Bresson, L. Vio, T. Vercouter and F. Chartier, *Anal. Chim. Acta*, 2015, **885**, 57.

24 G. Grindlay, S. Maestre, L. Gras and J. Mora, *J. Anal. At. Spectrom.*, 2006, **21**, 1403.

25 I. Kálomista, A. Kéri and G. Galbács, *Talanta¸* 2017, **172**, 147.

26 K-S Ho, W-W Lee and W-T Chan, *J. Anal. At. Spectrom.*, 2015, **30**, 2066.

27 F. Laborda, J. Jiménez-Lamana, E. Bolea and J.R. Castillo, *J. Anal, At. Spectrom.*, 2013, **28**, 1220.

28 G. Grindlay, S. Alavi and J. Mostaghimi, *J. Anal. At. Spectrom.*, 2020, **35**, 2956.

29 G. Grindlay, L. Gras, J. Mora and M.T.C. de Loos-Vollebregt, *Spectrochim. Acta B, 2008,* **63**, 234.

30 G. Grindlay, L. Gras, J. Mora and M.T.C. de Loos-vollebregt, *Spectrochim. Acta B*, 2016, **115**, 8.

31 R. Serrano, G. Grindlay, L. Gras and J. Mora, *Spectrochim. Acta B, 2021,* **177**, 106070.

32 H. Wiltsche, M. Winkler and P. Tirk, *J. Anal. At. Spectrom.*, 2015, **30**, 2223.

33 D. Cardinal, L.Y. Alleman, J. de Jong, K. Ziegler and L. André, *J. Anal. At. Spectrom.,* 2003, **18**, 213.

34 F. Laborda, A.C. Gimenez-Ingalaturre, E. Bolea and J.R. Castillo, *Spectrochim Acta B,* 2020, **169**, 105883.